01 Jan 1996

Transient and Dynamic Average-Value Modeling of Synchronous Machine Fed Load-Commutated Converters

Keith Corzine
Missouri University of Science and Technology

S. D. Sudhoff

H. J. Hegner

D. E. Delisle

TRANSIENT AND DYNAMIC AVERAGE-VALUE MODELING OF SYNCHRONOUS MACHINE FED LOAD-COMMUTATED CONVERTERS

S.D. Sudhoff, Member, K.A. Corzine, Student Member
School of Electrical Engineering
University of Missouri - Rolla

H.J. Hegner, Member, D.E. Delisle, Member
Naval Surface Warfare Center
Annapolis Detachment, Carderock Division

Abstract - **A new average-value model of a synchronous machine fed load-commutated converter is set forth in which the stator dynamics are combined with the dc link dynamics. This model is shown to be extremely accurate in predicting system transients and in predicting frequency-domain characteristics such as the impedance looking into the synchronous machine fed load-commutated converter. The model is verified against a detailed computer simulation and against a hardware test system, thus providing a three-way comparison. The proposed model is shown to be much more accurate than models in which the stator dynamics are neglected.**

I. Introduction

Synchronous machine fed load commutated converters are commonly used in a wide variety of applications including high-power dc supplies, excitation systems of large electric generators, variable-speed electric drive systems, aircraft power systems, and shipboard and submarine power systems. Computer simulation of these systems provides design evaluation and insight, and allows transient and contingency conditions to be studied without risk to hardware.

However, detailed computer simulations are computationally intense since the switching of each semiconductor must be taken into account. The presence of fast stator electrical dynamics and slow mechanical dynamics compounds the problem. In the event that mechanical dynamics are particularly long-lived, or when a large number of runs are required as necessary when generating frequency response characteristics or when performing Monte Carlo studies on a range of transient events, the computation time can be on the order of hours, or, in extreme cases, days. These difficulties have led to the simulation of these systems in average-value form. In this type of simulation, only the average-value or fundamental component of the waveforms are represented, and state variables are constant in the steady-state. Since the fast electrical transients are not periodically excited by the switching of the semiconductors, simulation algorithms for stiff system such as Gear's method become effective resulting in computationally efficient simulations.

96 WM 133-9 EC A paper recommended and approved by by the IEEE Electric Machinery Committee of the IEEE Power Engineering Society for presentation at the 1996 IEEE/PES Winter Meeting, January 21-25, 1996, Baltimore, MD. Manuscript submitted July 26, 1995; made available for printing December 8, 1995.

In addition, the fact that the state variables are constant in the steady-state makes linearization straightforward, and allows the automatic linearization capabilities featured by many simulation languages to be used to instantaneously determine frequency-domain characteristics. This is particularly important in the case of dc power systems in which many of the loads have dc/dc converter front ends. These loads are constant power in nature and thus as the dc bus voltage rises (falls) the current into the load decreases (increases). This destabilizing effect, known as negative impedance instability [1], is readily studied through the use of average-value models.

Recently, a highly accurate reduced-order average-value model of synchronous machine fed load-commutated converter was set forth [2-4]. Although average-value models are typically not used for harmonic analysis, the model set forth in [2-4] can in fact be used to reconstruct the waveform level details which typically require the use of detailed computer simulations [3]. However, though shown to yield excellent results in the steady-state, the model set forth in [2-4] neglects the stator dynamics of the synchronous machine and therefore does not accurately portray fast electrical transients. This paper sets forth an average-value model which is identical to the model set forth in [2-4] in the steady-state, but includes the effect of stator dynamics. The model is verified against a detailed computer simulation and against a hardware test system, thus providing a three way comparison in both the time and frequency domains. The proposed model is extremely useful in conducting large-disturbance average-value system simulations as well as in determining the frequency response characteristics of synchronous machine fed load-commutated converters.

II. System Description

A synchronous machine fed load-commutated converter is depicted in Fig. 1. Therein v_{as}, v_{bs}, and v_{cs} denote the

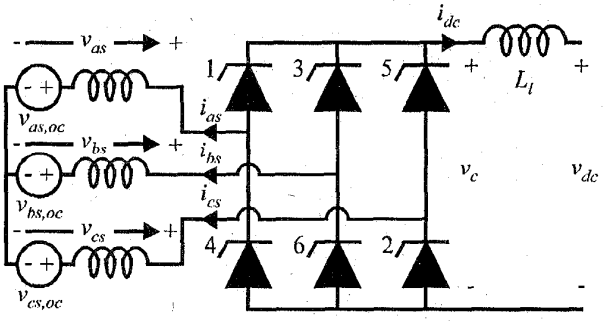

Fig. 1. Synchronous machine fed load-commutated converter.

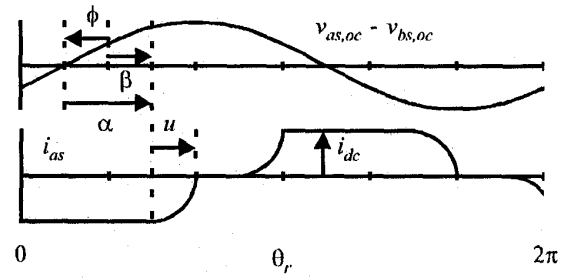

Fig. 2. Operation of synchronous machine fed load-commutated converter.

line-to-neutral voltages and i_{as}, i_{bs}, and i_{cs} the stator currents, which are positive into the machine. The converter consists of six thyristors valves labeled 1 through 6. If a voltage is applied to the gate of a thyristor, the thyristor is said to be gated on, regardless of whether or not it conducts. A valve is said to fire when it first conducts after being gated on. The converter voltage is denoted v_c, the dc link output voltage v_{dc}, and the dc link current i_{dc}.

Fig. 2 illustrates the b- to a-phase line-to-line open-circuit voltage of the synchronous machine and the a-phase current versus electrical rotor position for Mode 1 operation [5] (the mode considered throughout this paper). Angles of interest include β, the firing angle relative to rotor position, α, the firing angle relative to the back emf, ϕ, the angle of the back emf to relative to rotor position, and u, the commutation angle.

The synchronous machine model used is based on Park's transformation [6]. The q- and d-axis equivalent circuits are illustrated in Fig. 3. Therein m and n designate the number of damper circuits used to represent the machine. In Fig. 3 and throughout this paper (unless otherwise noted), all rotor quantities have been referred to the stator by the appropriate turns ratio. The q- and d-axis variables are related to the machine variables by

$$f^r_{qd0s} = K^r_s(\theta_r) f_{abcs} \tag{1}$$

where

$$f^r_{qd0s} = \left[f^r_{qs} \;\; f^r_{ds} \;\; f_{0s} \right]^T, \tag{2}$$

$$f_{abcs} = \left[f_{as} \;\; f_{bs} \;\; f_{cs} \right]^T, \tag{3}$$

f may be a voltage, current, or flux linkage and

$$K^r_s(\theta_r) = \frac{2}{3} \begin{bmatrix} \cos\theta_r & \cos(\theta_r - \frac{2\pi}{3}) & \cos(\theta_r + \frac{2\pi}{3}) \\ \sin\theta_r & \sin(\theta_r - \frac{2\pi}{3}) & \sin(\theta_r + \frac{2\pi}{3}) \\ \frac{1}{2} & \frac{1}{2} & \frac{1}{2} \end{bmatrix}^T. \tag{4}$$

Since a neutral connection is not present $f_{0s} = 0$.

III. Model Structure

The objective of this paper is set forth a highly accurate transient model of a synchronous machine fed load-commutated converter for use in system analysis and design. Before considering the details of this model, it is appropriate to consider the use of such a model within a system context. Fig. 4 illustrates the simulation architecture of a system utilizing a synchronous machine fed load-commutated converter. Since an average-value model is sought, all the variables depicted in Fig. 4 should be interpreted as average-values.

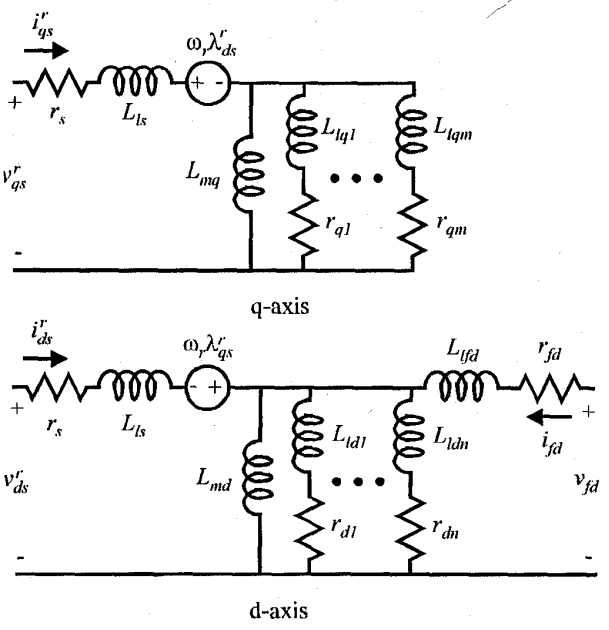

Fig. 3. Synchronous machine equivalent circuit.

As can be seen, a reduced-order synchronous machine model plays a central role in the system simulation. Although a reduced-order model is used in this block, stator dynamics will in fact be represented. In particular, the stator dynamics will be incorporated into the dc link dynamics. Outputs of the synchronous machine model include the electromagnetic torque T_e and q- and d-axis sub-transient flux linkages λ''_q and λ''_d. Inputs to this block include the field voltage v_{fd}, the electrical rotor speed ω_r, and the q- and d-axis stator currents i^r_{qs} and i^r_{ds}. Techniques for the formulation of reduced-order synchronous machine models are well established [7]. In the reduced-order model it is convenient to use the q-axis rotor flux linkages, d-axis rotor flux linkages, and field flux linkage as state variables. The time derivatives of these variables may be expressed as

$$p\lambda_{qi} = -r_{qi} i_{qi} \quad 1 \le i \le m \tag{5}$$

$$p\lambda_{di} = -r_{di} i_{di} \quad 1 \le i \le n \tag{6}$$

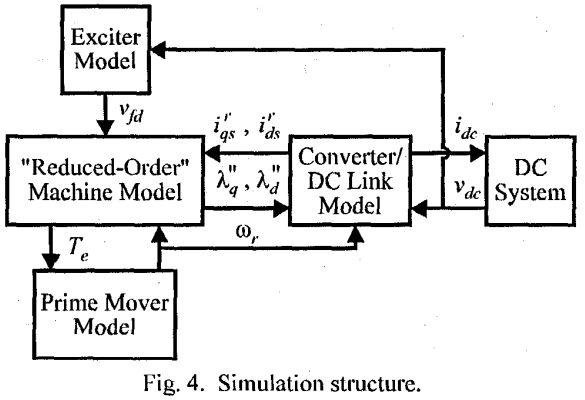

Fig. 4. Simulation structure.

$$p\lambda_{fd} = v_{fd} - r_{fd} i_{fd} \tag{7}$$

wherein the currents necessary to calculate the derivatives may be determined using

$$i_{qi} = \frac{\lambda_{qi} - L_{mq} i_{mq}}{L_{lqi}} \quad 1 \le i \le m \tag{8}$$

$$i_{di} = \frac{\lambda_{di} - L_{md} i_{md}}{L_{ldi}} \quad 1 \le i \le n \tag{9}$$

$$i_{fd} = \frac{\lambda_{fd} - L_{md} i_{md}}{L_{lfd}} \tag{10}$$

In (8-10) the magnetizing currents i_{mq} and i_{md} (not to be confused with the currents in the m'th damper circuits i_{qm} and i_{dm}) are calculated using

$$i_{mq} = i_{qs}^r + \frac{\sum_{i=1}^{m} \frac{\lambda_{qi}}{L_{lqi}} - i_{qs}^r L_{mq} \sum_{i=1}^{m} \frac{1}{L_{lqi}}}{1 + L_{mq} \sum_{i=1}^{m} \frac{1}{L_{lqi}}} \tag{11}$$

$$i_{md} = i_{ds}^r + \frac{\sum_{i=1}^{n} \frac{\lambda_{di}}{L_{ldi}} + \frac{\lambda_{fd}}{L_{lfd}} - i_{ds}^r L_{md} \left(\frac{1}{L_{lfd}} + \sum_{i=1}^{n} \frac{1}{L_{ldi}} \right)}{1 + L_{md} \left(\frac{1}{L_{lfd}} + \sum_{i=1}^{n} \frac{1}{L_{ldi}} \right)} \tag{12}$$

Finally, the electromagnetic torque is calculated as

$$T_e = \frac{3}{2}\frac{P}{2}(\lambda_{md} i_{mq} - \lambda_{mq} i_{md}) \tag{13}$$

where

$$\lambda_{mq} = L_{mq} i_{mq} \tag{14}$$

$$\lambda_{md} = L_{md} i_{md} \tag{15}$$

The calculation of the subtransient flux linkages from the rotor states is set forth in the following section.

The exciter and prime mover models are a function of the specific types of exciter and prime mover installed. This paper will focus on the converter / dc link model. As can be seen the inputs to this model are the q- and d- axis sub transient flux linkages λ_q'' and λ_d'' and the converter voltage v_{dc}; outputs include the dc link current i_{dc} and the average q- and d- axis stator currents i_{qs}^r and i_{ds}^r.

IV. Mathematical Development

The first step in the formulation of the converter/dc link model is the formulation an expression for the average converter voltage. The opening and closing of the thyristor valves result in a periodic transient which is of high frequency when compared to the dominant rotor time constants of the machine. For this reason, it is convenient to work with the subtransient synchronous machine model. In terms of subtransient quantities, the stator flux linkages equations may be expressed

$$\lambda_{qs}^r = L_q'' i_{qs}^r + \lambda_q'' \tag{16}$$

$$\lambda_{ds}^r = L_d'' i_{ds}^r + \lambda_d'' \tag{17}$$

where L_q'' and L_d'' are subtransient inductances defined by

$$L_q'' = L_{ls} + \left(\frac{1}{L_{mq}} + \sum_{i=1}^{m} \frac{1}{L_{ldi}} \right)^{-1} \tag{18}$$

$$L_d'' = L_{ls} + \left(\frac{1}{L_{md}} + \frac{1}{L_{lfd}} + \sum_{i=1}^{n} \frac{1}{L_{ldi}} \right)^{-1} \tag{19}$$

and λ_q'' and λ_d'' are subtransient flux linkages given by

$$\lambda_q'' = (L_q'' - L_{ls}) \sum_{i=1}^{m} \frac{\lambda_{qi}}{L_{lqi}} \tag{20}$$

$$\lambda_d'' = (L_d'' - L_{ls}) \left(\frac{\lambda_{fd}}{L_{lfd}} + \sum_{i=1}^{n} \frac{\lambda_{di}}{L_{ldi}} \right) \tag{21}$$

The operation of the synchronous machine fed load-commutated converter system is symmetric in that the q- and d-axis variables are periodic in $\pi/3$ radians. It is convenient to define six switching intervals which are defined such that switching interval x begins when thyristor x starts to conduct and ends when thyristor x+1 (modulus 6) begins to conduct. Consider switching interval 3 which begins when valve 3 is fired and ends when valve 4 is fired. During this interval the average converter voltage is given by

$$\bar{v}_c = \frac{3}{\pi} \int_{\pi/3}^{2\pi/3+\beta} (v_{bs} - v_{cs}) d\theta_r. \tag{22}$$

If stator resistance is neglected, then

$$v_{bs} = p\lambda_{bs} \tag{23}$$

$$v_{cs} = p\lambda_{cs} \tag{24}$$

where p denotes differentiation with respect to time. Substituting (23) and (24) into (22) yields

$$\bar{v}_c = \frac{3}{\pi} \omega_r (\lambda_{bs} - \lambda_{cs}) \Big|_{\pi/3+\beta}^{2\pi/3+\beta}. \tag{25}$$

To evaluate (25), it is necessary to find $\lambda_{bs} - \lambda_{cs}$ at each limit of integration. In order to accomplish this, it is first necessary to specify the stator currents at each limit of integration. In particular, when valve 3 fires only valves 1 and 2 are conducting, thus

$$i_{abcs}|_{\theta_r = \beta + \pi/3} = \begin{bmatrix} -i_{dc} & 0 & i_{dc} \end{bmatrix}^T \tag{26}$$

and at instant valve 4 fires only valves 2 and 3 are conducing; therefore

$$i_{abcs}|_{\theta_r = \beta + 2\pi/3} = \begin{bmatrix} 0 & -(i_{dc} + \Delta i_{dc}) & (i_{dc} + \Delta i_{dc}) \end{bmatrix}^T. \tag{27}$$

In (27), Δi_{dc} denotes the change in the dc current between the beginning of switching interval 3 and the beginning of switching interval 4. To complete the derivation of an expression for the average converter voltage, λ_{bs} and λ_{cs} are found by transforming (26) or (27), depending on the point of evaluation, into the rotor reference frame. The values of i_{qs}^r and i_{ds}^r are then substituted into (16) and (17) to determine λ_{qs}^r and λ_{ds}^r at each boundary. The boundary values of λ_{qs}^r and λ_{ds}^r are then transformed back into machine variables to calculate $\lambda_{bs} - \lambda_{cs}$ at each limit of integration. After considerable manipulation this sequence of operations yields

$$\bar{v}_c = \frac{3\sqrt{3}}{\pi} \omega_r \left(-\lambda_q'' \sin\beta + \lambda_d'' \cos\beta \right) - \frac{3}{\pi} \omega_r L_c(\beta) i_{dc} - \frac{3}{\pi} \omega_r L_t(\beta) \Delta i_{dc} \tag{28}$$

where

$$L_c(\beta) = \frac{1}{2}(L_q'' + L_d'') + (L_d'' - L_q'') \sin(2\beta + \frac{\pi}{6}) \tag{29}$$

and

$$L_t(\beta) = L_q'' + L_d'' + (L_d'' - L_q'') \sin(2\beta - \frac{\pi}{6}). \tag{30}$$

Equation (29) defines the commutating inductance of the synchronous machine, as set forth in [2]. Equation (30) defines the transient commutating inductance of the synchronous machine.

It is convenient to define the subtransient voltages as

$$e_q'' = \omega_r \lambda_d'' \tag{31}$$

$$e_d'' = -\omega_r \lambda_q'' \tag{32}$$

whereupon (28) may be expressed

$$\bar{v}_c = \frac{3\sqrt{3}}{\pi} E \cos\alpha - \frac{3}{\pi}\omega_r L_c(\beta) i_{dc} - \frac{3}{\pi}\omega_r L_l(\beta)\Delta i_{dc} \tag{33}$$

where E is the magnitude of the subtransient voltage given by

$$E = \sqrt{\left(e_q''\right)^2 + \left(e_d''\right)^2}, \tag{34}$$

α is the phase delay relative to the back emf given by

$$\alpha = \beta + \phi \tag{35}$$

and ϕ is the phase of the subtransient voltage defined by

$$\phi = \text{angle}(e_q'' - j e_d''). \tag{36}$$

Representing the dc current i_{dc} by its average value $\bar{i}_{dc}$, the average value of the derivative of the current as

$$p\bar{i}_{dc} = \frac{\pi}{3\omega_r}\Delta i_{dc}, \tag{37}$$

and the voltage drop due to the stator resistance as $2r_s\bar{i}_{dc}$, (33) becomes

$$\bar{v}_c = \frac{3\sqrt{3}E}{\pi}\cos\alpha - \frac{3}{\pi}\omega_r L_c(\beta)\bar{i}_{dc} - 2r_s\bar{i}_{dc} - L_l(\beta)p\bar{i}_{dc}. \tag{38}$$

There are several interesting features of (38). First, there is a converter voltage drop due the stator dynamics associated with the changing dc link current. Another interesting feature of (38) is that both the commutating inductance and the transient commutating inductance are functions of firing angle β. Thus, the synchronous machine rectifier can be viewed as a voltage behind a RL source, where the voltage, the resistance (represented by the stator resistance and the commutating inductance), and inductance are all functions of phase delay. Since β is in itself a function of the subtransient flux linkages and the dc link current, both the steady-state and transient characteristics of the synchronous machine fed load-commutated converter are dependent upon operating point.

Fig. 5 depicts the commutating inductance and transient commutating reactance for a synchronous machine in which the q- and d- axis subtransient inductances are 2.78 mH and 1.95 mH, respectively. As can be seen, the commutating inductance varies from a value less than the d-axis subtransient inductance to a value greater than the q-axis subtransient inductance, a factor of 2.1:1. The transient commutating inductance, which has been divided by 2 in Fig. 5, varies from twice the d-axis subtransient inductance to twice the q-axis subtransient inductance.

In order to complete the converter / dc link model, note that the dc link dynamics are governed by

$$pi_{dc} = \frac{v_c - v_{dc} - r_l i_{dc}}{L_l} \tag{39}$$

which, in average value form, may be expressed

$$p\bar{i}_{dc} = \frac{\bar{v}_c - \bar{v}_{dc} - r_l\bar{i}_{dc}}{L_l} \tag{40}$$

Combining (38) and (40) yields

$$p\bar{i}_{dc} = \frac{\frac{3\sqrt{3}}{\pi}E\cos\alpha - \bar{v}_{dc} - (r_l + \frac{3}{\pi}\omega_r L_c(\beta))\bar{i}_{dc}}{L_l + L_l(\beta)}. \tag{41}$$

The remaining relationships necessary to formulate the converter /dc link model are the calculation of the firing angle β and the

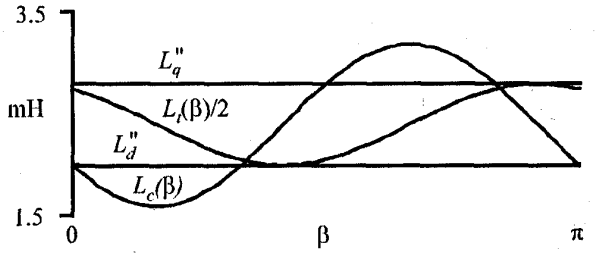

Fig. 5. Commutating and transient inductance versus firing angle.

calculation of the average q- and d-axis currents. The method whereby these quantities are determined is as derived in [2] and so will not be proven herein. However, the principal results are discussed below for completeness.

The calculation of β is directly tied to the method used to generate the logic signals used to turn on the thyristor valves. There are numerous methods whereby this can be accomplished. For example, these signals may be established by filtering the terminal voltages of the synchronous machine and using the cosine-comparitor control strategy [8]. Alternatively, the firing signals may be based upon sensed rotor position using Hall-effect devices, optical encoders, or sensor windings. Whatever the method, the signals from which the gating logic are derived can be mathematically related to rotor position. In particular, the commanded firing angle relative to rotor position, denoted β_c, can be specified. This angle is defined such that valve 3 is gated on when $\theta_r = \beta_c + \pi/3$.

Because a valve may be gated on before it can conduct, there is a distinction between β and β_c. The minimum firing angle for which a valve will fire when gated on is denoted $\beta_{\min}$. This angle is found by solving

$$f_{\min}(\beta_{\min}) = 0 \tag{42}$$

where

$$f_{\min}(\beta_{\min}) = \sqrt{3}\,(\lambda_q''\cos\beta_{\min} + \lambda_d''\sin\beta_{\min}) + 2\bar{i}_{dc}(L_q'' - L_d'')\sin(2\beta_{\min} - \tfrac{\pi}{3}). \tag{43}$$

If β_c is less than $\beta_{\min}$, the thyristors, while gated on at the specified rotor position, will not fire until the position corresponding to $\beta_{\min}$. Therefore, the firing angle is given by

$$\beta = \max(\beta_{\min}, \beta_c). \tag{44}$$

Calculation of the average q- and d-axis currents is a multi-step procedure. First, the intermediate variable K is given by

$$K = \sqrt{3}\,(-\lambda_q''\sin\beta + \lambda_q''\cos\beta) + \left[(L_d'' - L_q'')\cos(2\beta + \frac{2\pi}{3}) - \frac{1}{2}(L_q'' + L_d'')\right]\bar{i}_{dc}. \tag{45}$$

Next, the commutation angle u is found by solving

$$0 = K - \sqrt{3}\left[-\lambda_q''\sin(\beta + u) + \lambda_d''\cos(\beta + u)\right] - \left[(L_q'' - L_d'')\sin(2\beta + 2u - \frac{2\pi}{3}) + \frac{1}{2}(L_q'' + L_d'')\right]\bar{i}_{dc}. \tag{46}$$

The average-value of the q- and d- axis currents is broken into conduction and commutation components. The conduction component of the q- and d-axis currents may be expressed as

$$\bar{i}^{\,r}_{qs,cond} = \frac{2\sqrt{3}}{\pi}\bar{i}_{dc}\left[\cos(\beta+\tfrac{2\pi}{3}) - \cos(\beta+u+\tfrac{\pi}{3})\right] \quad (47)$$

$$\bar{i}^{\,r}_{ds,cond} = \frac{2\sqrt{3}}{\pi}\bar{i}_{dc}\left[\sin(\beta+\tfrac{2\pi}{3}) - \sin(\beta+u+\tfrac{\pi}{3})\right] \quad (48)$$

The a-phase and q- and d-axis currents must be expressed in the commutation interval following the firing of valve 3 in order to compute the commutation component of the q- and d-axis currents. During this interval, the a-phase current is given by

$$i_{as}(\theta_r) = \frac{K+\sqrt{3}\left(\lambda''_q\sin(\tilde{\theta}_r+\beta) - \lambda''_d\cos(\tilde{\theta}_r+\beta)\right)}{(L''_q+L''_d) - (L''_q-L''_d)\cos(2\tilde{\theta}_r+2\beta)} - \frac{\left[(L''_q-L''_d)\cos(2\tilde{\theta}_r+2\beta-\frac{2\pi}{3}) + \frac{1}{2}(L''_q+L''_d)\right]\bar{i}_{dc}}{(L''_q+L''_d) - (L''_q-L''_d)\cos(2\tilde{\theta}_r+2\beta)}. \quad (49)$$

In (38), $\tilde{\theta}_r$ is the electrical rotor position offset such that valve 3 fires when $\tilde{\theta}_r = 0$. It follows that the q- and d- axis currents may be expressed

$$i^r_{qs}(\tilde{\theta}_r) = \frac{2\sqrt{3}}{\pi}\left[-i_{as}(\tilde{\theta}_r)\sin(\tilde{\theta}_r+\beta) - i_{dc}\sin(\tilde{\theta}_r+\beta+\frac{\pi}{3})\right] \quad (50)$$

$$i^r_{ds}(\tilde{\theta}_r) = \frac{2\sqrt{3}}{\pi}\left[i_{as}(\tilde{\theta}_r)\cos(\tilde{\theta}_r+\beta) + \bar{i}_{dc}\cos(\tilde{\theta}_r+\beta+\frac{\pi}{3})\right]. \quad (51)$$

Using (49-51), the commutation component of the average q-and d-axis currents is given by

$$\bar{i}^{\,r}_{qs,com} = \frac{u}{4\pi}\left[i^r_{qs}(0) + 4i^r_{qs}(\tfrac{u}{4}) + 2i^r_{qs}(\tfrac{u}{2}) + 4i^r_{qs}(\tfrac{3u}{\pi}) + i^r_{qs}(u)\right] \quad (52)$$

$$\bar{i}^{\,r}_{ds,com} = \frac{u}{4\pi}\left[i^r_{ds}(0) + 4i^r_{ds}(\tfrac{u}{4}) + 2i^r_{ds}(\tfrac{u}{2}) + 4i^r_{qs}(\tfrac{3u}{4}) + i^r_{qs}(u)\right] \quad (53)$$

whereupon the average q- and d- axis currents may be expressed

$$\bar{i}^{\,r}_{qs} = \bar{i}^{\,r}_{qs,com} + \bar{i}^{\,r}_{qs,cond} \quad (54)$$

$$\bar{i}^{\,r}_{ds} = \bar{i}^{\,r}_{ds,com} + \bar{i}^{\,r}_{ds,cond}. \quad (55)$$

For the purposes of time domain analysis it is necessary to calculate the time derivatives of the state variables in terms of input variables and the state variables. Computationally, the first calculation is that of the q- and d-axis subtransient flux linkages (λ''_q and λ''_d) from the rotor states using (20-21). Then, using the subtransient flux linkages and the dc link current i_{dc} the firing angle relative to rotor position β and the fast average of the q- and d-axis currents i^r_{qs} and i^r_{ds} may be found using the procedure set forth in (42-55). Based on the stator currents and field voltage (in input) the time derivatives of the rotor states may be found using (11-12), (8-10), and finally (5-7) and the torque may be calculated using (14-15) and then (15). Following this sequence of operations, all variables required to calculate the derivative of the dc link current using (41) are available.

IV. Verification

The test system illustrated in Fig. 6 was used to verify the time domain performance of the average-value and detailed simulations. The synchronous machine parameters were obtained using standstill frequency response [9] and are listed in Table 1, wherein all rotor parameters have been referred to the stator by the appropriate turns

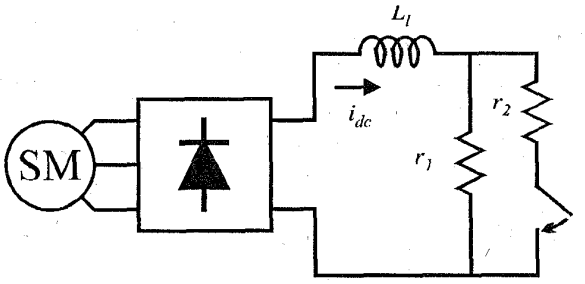

Fig. 6. System configuration for time-domain test.

ratio. The dc link inductor has an inductance of 1.19 mH and a series resistance of 0.32 Ω, and r_1 and r_2 were 21.0 and 4.04 Ω, respectively. Figs. 7-8 illustrate the transient behavior of the system when operated at a speed of 377 rad/s and with a fixed applied field voltage of 19.5 V as the switch is closed. Variables depicted include the dc current i_{dc} and the actual (not referred to the stator) field current i_{fd} as measured, as predicted by the detailed simulation, and as predicted by the average-value simulation.

As can be seen, immediately following the closing of the switch, the dc current rises quite rapidly. The field current rises in order to maintain constant flux. As the field and damper currents decay, the flux-level in the machine drops; this reduces the back emf which in turn causes the dc link current to decrease.

Although the detailed computer simulation does not exactly match the observed results, it nevertheless portrays the salient features of the transient event. Since the machine was not heavily saturated during the study, the most likely cause for the discrepancies which due exist are the representation of the rotor windings. In particular, it is believed that a better comparison could be obtained by including the effect of mutual leakage inductance between the field and damper windings [10], although this

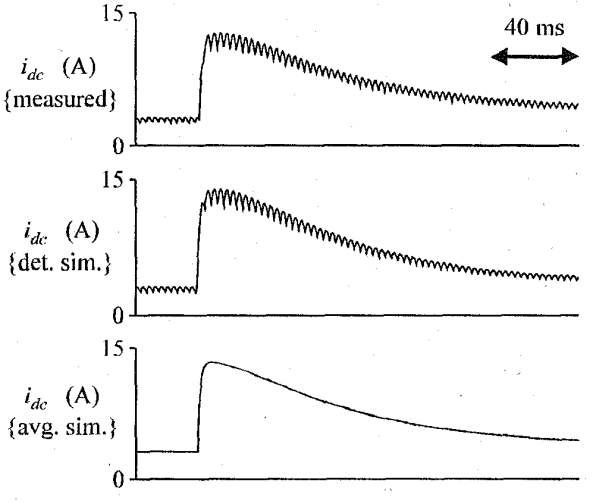

Fig. 7. DC link current during step increase in load as measured, as predicted by detailed simulation, and as predicted by average-value simulation.

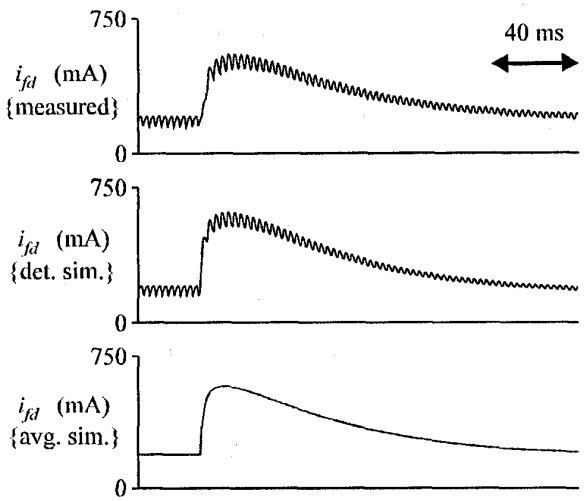

Fig. 8. Field current during step increase in load as measured, as predicted by detailed simulation, and as predicted by average-value simulation.

conclusion has not been verified experimentally. As can be seen, the average-value model captures the salient features of the transient as well as the detailed model, with the exception of harmonics. Due to the fact that the stator transients are incorporated into the average-value model, even the fast transient governing the rise of the dc link current is accurately portrayed.

TABLE I. 3.7 kW SYNCHRONOUS MACHINE PARAMETERS			
$r_s = 382\ \text{m}\Omega$	$L_{ls} = 1.12$ mH	$L_{mq} = 24.9$ mH	$L_{md} = 39.3$ mH
$r_{d1} = 140\ \Omega$	$L_{ld1} = 9.87$ mH	$r_{q1} = 5.07\ \Omega$	$L_{lq1} = 4.21$ mH
$r_{d2} = 1.19\ \text{k}\Omega$	$L_{ld2} = 4.91$ mH	$r_{q2} = 1.06\ \Omega$	$L_{lq2} = 3.5$ mH
$r_{d3} = 1.58\ \Omega$	$L_{ld3} = 4.52$ mH	$r_{q3} = 447\ \text{m}\Omega$	$L_{lq3} = 26.2$ mH
$r_{fd} = 112\ \text{m}\Omega$	$L_{lfd} = 1.53$ mH	$N_s / N_{fd} = 0.0269$	$P = 4$

In the design of dc power systems, such as those found on ships, spacecraft, electric vehicles, and aircraft, impedance characteristics of both the sources and loads must be compatible if system and load stability are to be ensured [11]. Therefore, it is important that the average-value model accurately predicts the impedance characteristics of the synchronous machine fed load-commutated converter.

The calculation of the impedance characteristic using the average-value model is quite straightforward. In particular, since the model has state variables which are constant in the steady-state, it may be linearized in order to determine the small signal transfer function between Δv_{dc} and $-\Delta i_{dc}$, which is the impedance looking into the converter. Once the model has been coded, these steps can be automatically conducted by most state-variable based simulation languages [12].

The measurement of the impedance was conducted using the configuration illustrated in Fig. 9. Therein, switch S is switched at

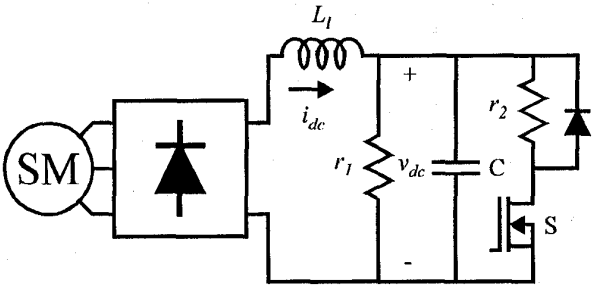

Fig. 9. System configuration for frequency-domain test.

the frequency of interest with a 50 % duty cycle. The parameters used were $r_1 = 12.06\ \Omega$, $r_2 = 43.09\ \Omega$, and C = 2.28 μF. The current i_{dc} and voltage v_{dc} are then captured on a digital oscilloscope and the waveforms are processed (by computing the amplitude and phase of the perturbation to these quantities) in order to arrive at the impedance. The calculation of the impedance characteristic from the detailed simulation was accomplished by simulating the system shown in Fig. 9, and processing the waveforms in exactly the same way as the measured waveforms were processed. The average-value model impedance calculations were conducted by automatic linearization of the time-domain model about an average resistive load of 10.74 Ω (the algebraic mean between r_1 and the parallel combination of r_1 and r_2).

Figs. 10 and 11 depict the magnitude and phase of the impedance looking into the converter as measured, as predicted by the detailed computer simulation, as predicted by the average-value model as set forth herein, and as predicted by an reduced-order average-value model in which the stator dynamics are not represented [2-4]. As can be seen, there is agreement between the measured impedance, the impedance calculated by the average-value model, and the impedance calculated by the detailed model set forth herein. It is also apparent that neglecting the stator transients as in [2-4] can lead to a large error in the calculated impedance at mid-to-high frequencies.

Before concluding, it is appropriate to discuss the computational aspects of the average value model. When performing time domain studies such as those illustrated in Fig. 7-8, the average-value model, which is represented mathematically as a set of differential equations, may be used with any integration algorithm. However, since there is generally a large spread in eigenvalues (the dc link current being associated with a very fast time constant while the rotor states are governed by slow time constants), integrations methods designed for stiff systems (such as Gear's method) can be effectively used, and in fact were used in the studies illustrated herein. When performing linearized frequency response, Gear's method is also useful in performing the time domain simulation required in order to predict the steady-state operating point about which the system is linearized. After the initial condition is established, the input and state variables are numerically perturbed and the resulting disturbances in the derivatives of the state variables are observed. From this information it is possible to calculate the A,

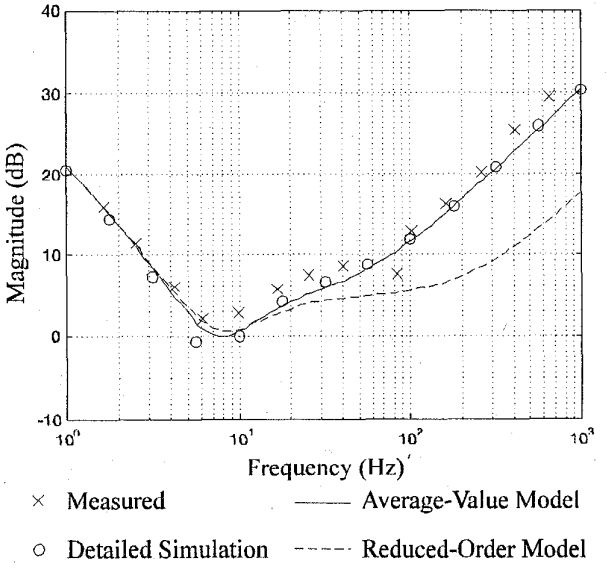

Figure 10. Impedance characteristic of synchronous machine fed load-commutated converter.

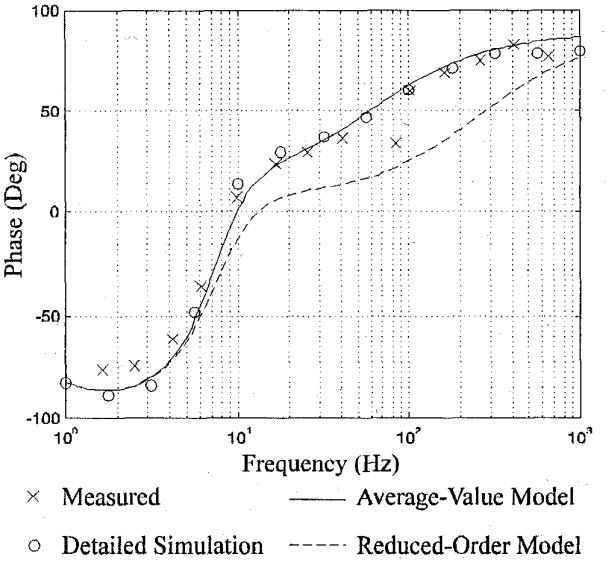

Figure 11. Impedance characteristic of synchronous machine fed load-commutated converter.

B, C, and D matrices which describe the linearized system model. These matrices are then used to calculated the frequency response. In the case of the detailed simulation the calculation of the frequency response is done on a frequency-by-frequency basis as previously described. The calculation of the input impedance using the average value model is much more efficient; it was found that whereas the detailed model requires 5.6 h to calculate the input impedance characteristic the average-value model only required 6.2 s on a Sun Spark 10 workstation.

V. Summary

An average-value model of a synchronous machine fed load-commutated converter has been set forth. This model possesses the unique feature that the synchronous machine stator dynamics are incorporated into the dc link dynamics. The predictions of the model have been compared to measurements obtained from a hardware test system and to the predictions of a detailed simulation, with good agreement. In addition, it has been shown that average-value models in which the stator dynamics are completely neglected can yield considerable error when predicting frequency response, particularly in the mid-to-high frequency range.

VII. Acknowledgments

The authors thank the U.S. Navy Advanced Surface Machinery Program, P.C. Krause and Associates, and the University of Missouri Research Board for their support of this work.

VIII. References

[1] R.D. Middlebrook, "Input Filter Considerations in Design and Application of Switching Regulators," IEEE Proc. IASAM, 1976.
[2] S.D. Sudhoff and O. Wasynczuk, "Analysis and Average-Value Modeling of Line-Commutated Converter - Synchronous Machine Systems," *IEEE Trans. on Energy Conversion*, Vol. 8, No. 1, March 1993, pp. 92-99.
[3] S. D. Sudhoff, "Waveform Reconstruction From the Average-Value Model of Line-Commutated Converter - Synchronous Machine Systems," *IEEE Trans. on Energy Conversion*, Vol. 8, No. 3, September 1993, pp. 411-417.
[4] S.D. Sudhoff, "Analysis and Average-Value Modeling of Line-Commutated Converter - Synchronous Machine Systems," *IEEE Trans. on Energy Conversion*, Vol. 8, No. 3, September 1993, pp. 404-410.
[5] R.L. Witzke, J.V. Kresser, and J.K. Dillard, "Influence of AC Reactance on Voltage Regulation of 6-Phase Rectifiers," *AIEE Transactions*, Vol. 72, July 1953, pp. 244-253.
[6] R.H. Park, "Two-Reaction Theory of Synchronous Machines - Generalized Method of Analysis - Part I," *AIEE Trans.*, Vol. 48, July 1929, pp. 716-727.
[7] P.C. Krause, *Analysis of Electric Machinery*, McGraw Hill, 1986.
[8] B.R. Pelly, *Thyristor Phase-Controlled Converters and Cycloconverters; Operation, Control, and Performance*, Wiley Interscience, New York, 1971.
[9] IEEE Std. 115A-1987.
[10] I. Kamwa and P. Viarouge, "On Equivalent Circuit Structures For Empirical Modeling of Turbine-Generators," *IEEE Transactions on Energy Conversion*, Vol. 9, No. 3, September 1994.
[11] PPD 802-6335721, SSN-21, "Combat System Direct Current Electric Power Interface", Department of the Navy, Washington D.C. 20362, April 30, 1987.
[12] ACSL Reference Manual, Edition 11.1, MGA Software, Concord MA 01742.

Scott D. Sudhoff received the BSEE, MSEE, and Ph.D. degrees at Purdue University in 1988, 1989, and 1991, respectively. He is currently an Assistant Professor at the University of Missouri - Rolla. His interests include electric machines, electric drive systems, power electronics, flexible ac transmission, and finite-inertia power systems.

Keith A. Corzine received the BSEE and MSEE degrees from the University of Missouri - Rolla in 1992 and 1994, respectfully, and is currently pursuing the Ph.D. degree. His interests include the design and analysis of electric machinery and electric drive systems. He has authored or co-authored four transactions papers in these areas.

Henry J. Hegner received the BSEE degree from Virginia Polytechnical Institute and State University in 1983 and MSEE degree from Purdue University in 1992. Mr. Hegner is employed within the Electrical Systems Department of the Machinery Research and Development Directorate at the Naval Surface Warfare Center in Annapolis, Maryland. For the past 16 years, Mr. Hegner has specialized in electrical systems and components for shipboard systems. He is currently a member of the U.S. Navy's Advanced Surface Machinery Programs (ASMP), where he is serving as Team Leader for the DC Zonal Electrical Distribution System and is a member of the Integrated Power System development teams.

Dana E. Delisle received the BSEE degree from the University of Massachusetts in 1984. He is employed within the Electrical System Division of the Naval Surface Warfare Center, Annapolis, Maryland. For the past 10 years he has specialized in dc electrical power systems for Navy shipboard electronic systems.